Using the Dynamic Energy Budget theory to evaluate the bioremediation potential of the polychaete Hediste diversicolor in an integrated multi-trophic aquaculture system

Helena Lopes Galasso, Sebastien Lefebvre, Catherine Aliaume, Bastien Sadoul, Myriam D. Callier

Using the Dynamic Energy Budget theory to evaluate the bioremediation potential of the polychaete *Hediste diversicolor* in an integrated multi-trophic aquaculture system

Helena Lopes Galasso[a,b*], Sébastien Lefebvre[c], Catherine Aliaume[d], Bastien Sadoul[a] and Myriam D. Callier[a*]

[a] MARBEC, Univ Montpellier, CNRS, Ifremer, IRD, Palavas-les-Flots, France

[b] CAPES Foundation, Ministry of Education of Brazil, Brasília, DF 70040-020, Brazil

[c] Université de Lille, Université Littoral Côte d'Opale, CNRS, Laboratoire d'Océanologie et Géosciences (UMR 8187 LOG), Station Marine de Wimereux, F-59000 Lille, France

[d] MARBEC, Univ Montpellier, CNRS, Ifremer, IRD, Montpellier, France

*Corresponding author at: MARBEC, Univ Montpellier, CNRS, Ifremer, IRD, chemin de Maguelone, F-34250 Palavas-les-Flots, France.

E-mail address: myriam.callier@ifremer.fr (M.D. Callier), helenagalasso@gmail.com (H. Galasso)

Abstract

Integrated Multi-Trophic Aquaculture (IMTA) systems have been designed to optimize nutrient and energy use, to decrease waste, and to diversify fish-farm production. Recently, the development of detritivorous aquaculture has been encouraged, as detrivores can consume organic particulate matter, reducing benthic eutrophication and the environmental footprint of aquaculture. To this end, the polychaete *Hediste diversicolor* is a promising species due to its broad feeding behaviour and its resistance in a wide range of environments. In this study, an existing Dynamic Energy Budget (DEB) model of *H. diversicolor* was used to predict the ragworm's metabolic processes in various environmental conditions and to estimate its bioremediation capacity in an aquaculture context. First, the scaled functional response (*f*) was calibrated in a 98-day growth experiment with two types of food (Fish faeces and Fish feed). Then, we further validated the model using data on the ammonia excretion and oxygen consumption of individuals fed with fish faeces at four different temperatures using the previously calibrated *f*. Overall, we found that the DEB model was able to correctly predict the experimental data ($0.51<MRE<0.80$). Lastly, different environmental scenarios of seawater temperatures and assimilation rates were compared. The bioremediation potential of *H. diversicolor* was estimated based on cumulated assimilation rates, which could represent 75-289 kg of fish waste $year^{-1}$ for a 100 m^2 ragworm farm (3700 ind. m^{-2}). These findings suggest that the DEB model is a promising tool for further IMTA development and management.

Keywords: DEB, deposit feeders, fish waste, metabolism, ragworm, semelparous, bioenergetics

1. Introduction

Fed aquaculture can impact ecosystems through the release of organic matter and dissolved nutrients (Hargrave, 2005). One way to minimize aquaculture waste is to develop Integrated Multi-Trophic Aquaculture (IMTA), in which organisms of different trophic levels are co-cultured on the same farm (Chopin et al., 2012). This type of aquaculture can include fed species (e.g. finfish or shrimp) as well as extractive species such as algae that can feed on dissolved inorganic waste generated by the fed species (Abreu et al., 2011; Erler et al., 2000) or filter-feeders and detritivores that can feed on generated organic waste (Jiang et al., 2013; Neori et al., 2004). In open water, particulate organic matter fluxes (faeces and uneaten feed) are mainly vertical (Filgueira et al., 2017) and may accumulate on the bottom sediment both within the farm site and close to it, inducing benthic eutrophication (Hargrave, 2005). The quantity and biochemical composition of the nutrients and organic matter released depends on the cultured species, the farm size, the feed composition, and the rearing conditions (Brigolin et al., 2010).

Using detritivore species in IMTA may improve the mineralization of organic matter through bioturbation processes (Hedman et al., 2011) and feeding (Cammen, 1980), thus preventing benthic eutrophication. The bioremediation potential of several detritivorous species has been evaluated, including fish (Katz et al., 2002; Porter et al., 1996), sea cucumbers (Cubillo et al., 2016; MacDonald et al., 2013; Nelson et al., 2012; Paltzat et al., 2008; Chary et al., 2020), sea urchins (Cook and Kelly, 2007; Orr et al., 2014) and polychaetes (Fang et al., 2017; Marques et al., 2017). Among polychaetes, *Hediste* (*Nereis*) *diversicolor* (O. F. Müller, 1776) has been widely studied (Gillet et al., 2008; Mermillod-Blondin et al., 2004). Similar to other Nereididae, this species plays an important ecological role by constructing burrows in sediment to create galleries.

Their bioturbation and ventilation activities promote nutrient fluxes between water and sediment, favouring the oxygenation of the sediment (Michaud et al., 2006) and enhancing organic matter mineralization and nutrient recycling (Heilskov and Holmer, 2001). Additionally, *H. diversicolor* can cope with a large range of environmental conditions, in terms of variation in organic matter loading, temperature and salinity (Kristensen, 1983; Ozoh and Jones, 1990). Moreover, its feeding behaviour is diversified: it is considered a detritivore, carnivore, herbivore, suspension feeder and even an optional filter feeder (Nielsen et al., 1995; Riisgård, 1994). More recently, the biomitigation activity of this species has been explored (Cubillo et al., 2016; Marques et al., 2017; Papaspyrou et al., 2010), and studies have demonstrated that individuals can grow significantly when fed on fish waste (Bischoff et al., 2009; Wang et al. 2019). Cubillo et al. (2016) and Marques et al. (2017) have also shown that *H. diversicolor* could assimilate particulate organic matter from fish farms, confirming its potential for IMTA. However, these studies were carried out under specific temperature and salinity conditions, making predicting the bioremediation capacity in other environmental conditions difficult. In this context, mechanistic models can be useful tools as they can simulate physiological and ecological processes under a large range of environmental conditions. Starting from empirical results in a limited number of environmental conditions, this modelling framework allows these results to be extrapolated in order to predict the metabolic responses of individuals in other environmental conditions (Reid et al., 2020). Bioenergetic models are based on the fluxes and conservation of energy in physiological processes, in which energy available for somatic growth is estimated as a result of feeding and excretion (Brett and Groves, 1979). The model chosen in this study was the Dynamic Energy Budget (DEB) model (Kooijman, 2010), which is based on the use of energy by an organism for physiological processes such as food

assimilation, growth, maintenance and reproduction. This model has been demonstrated to correctly model the lifecycle of a wide range of species, from bacteria to large mammals. The framework provided by the DEB theory allows the quantification of processes of interest for aquaculture (such as growth and feeding efficiency) and of increasing interest for IMTA (such as the bioremediation capacity of extractive species) (Reid et al., 2020, Chary et al., 2020). The associated DEB parameters for more than 2000 modelled species to date are available on the online platform Add-my-Pet (AmP) (www.bio.vu.nl/thb/deb/deblab/add_my_pet). Of these species, 7 are polychaetes, with the recent additions of *Arenicola marina* (De Cubber et al., 2019) and *Hediste diversicolor* (Lefebvre, 2019). These DEB model parameters for *H. diversicolor* can now be used to predict metabolic processes under different environmental conditions.

The aim of this study was to analyze the mitigation potential of deposit-feeding *H. diversicolor* in co-cultivation with finfish. The objectives were (1) to validate the DEB model using new datasets obtained through laboratory experiments on growth rates and ammonia excretion, as well as data on oxygen consumption published independently of the calibration procedure, (2) to evaluate the effects of seawater temperatures (5°C to 25°C) and assimilation rates (from *ad libitum* to half an *ad libitum* ration) on some life history traits of *H. diversicolor*, and (3) to quantify the bioremediation potential of *H. diversicolor* in different aquaculture contexts.

2. Material and methods

2.1. The DEB theory and the lifecycle of *H. diversicolor*

A general presentation of the DEB theory and its mathematical formulation is presented in 'Supplementary material' (see S1). To perform the DEB simulations for *H.*

diversicolor, we used the available parameters in the AmP database (Lefebvre, 2019) (Table 1), using an abj-model. Essentially, the DEB theory is based on the assumption that assimilated energy first enters a reserve compartment (E). A fixed fraction (κ) of the energy flux coming from the reserve is then utilized, first for somatic maintenance costs and the remaining part for growth of the structural volume (V). The other fraction (1-κ) is spent on maturation (E_H) in juveniles or on reproduction (E_R) in adults, after having paid the maturity maintenance costs (Figure 1). Acquisition processes (i.e. ingestion and assimilation) are linked to the organism's surface area, while somatic maintenance is proportional to its volume. In contrast to the standard version of the DEB model (std), the abj-model considers a metabolic acceleration between birth and metamorphosis (see S1). Consequently, we scaled maximum surface-specific assimilation ($\{\dot{p}_{Am}\}$) and energy conductance ($\dot{v}$) to the organism 's structural length between birth and metamorphosis, following Kooijman et al. (2011). Finally, as it is a semelparous species, *H. diversicolor* dies after its first reproduction (Olive and Garwood, 1981). Therefore, the maximum structural length L_m was the structural length of the animal that attains first reproduction. In DEB theory, authors refer to this reproductive strategy as 'suicide reproduction' (Kooijman, 2010).

The DEB model describes changes in the energy content of four state variables (E, V, E_H and E_R for adults), which cannot be measured directly. The volumetric structural length ($L=V^{1/3}$) can be approximated by the shape-corrected physical (observable) length (δ_M L_w). In this study, the length (cm) of the first three segments (L3: the combined length of the prostomium, peristomium and the first setiger) was used as the physical length, as this is more reliable than the total length in polychaetes. Wet weight (WW) was calculated as the sum of the wet mass of the structure and the wet mass of the reserve (see S1). The wet mass of the reproductive buffer was not included in the

143 WW calculation because it was considered negligible most of the time (GSI<3%, see
144 below).
145
146 **2.2. *H. diversicolor* growth performance in controlled environments**

147 **2.2.1. Sampling.** *H. diversicolor* individuals were collected in the wild in Arnel
148 Lagoon, on the French Mediterranean coast. The experiments were conducted in the
149 Ifremer marine aquaculture experimental station (Palavas-les-Flots, France). For the
150 oxygen and excretion experiments, individuals were acclimatized for 10 days (see
151 details below). For the growth experiment, *in vitro* reproduction was carried out in
152 October 2016 in order to begin with individuals of the same age. During the early larvae
153 stage (from 0 to 22 days), the polychaete offspring were fed with microalgae (*Chlorella*
154 *sp.*), which were cultured at the experimental station and can be ingested (this was
155 confirmed by microscopic observation of the gut content). Before the beginning of the
156 growth experiment, juveniles (from 22 to 113 days), were fed with fish faeces and
157 raised at temperatures ranging between 15°C and 18°C. This food was chosen because
158 fish farm waste is mainly composed of fish faeces and a varying proportion of uneaten
159 fish feed (Galasso et al., 2017).
160
161 **2.2.2 Growth rates.** The growth experiment was conducted on individuals when they
162 reached 113 days of age; the experiment lasted 98 days (February–April 2017). Two
163 types of feed were tested: faeces from farmed European seabass *Dicentrarchus labrax*
164 (Fish faeces) and commercial fish feed (Fish feed). The collection and preparation of
165 these are detailed in Galasso et al. (2017). The fish faeces were composed of 72%
166 organic matter (OM) (including 3% total organic nitrogen [TON] and 7% total lipids
167 [TL]), and 28% ash. The commercial fish feed was composed of 87% OM (including

168 7% TON and 12% TL) and 12% ash. Polychaetes were fed *ad libitum* (based on the
169 observation of leftover food in the tank) from 48 mg feed.ind^{-1}.d^{-1} to 85 mg.ind^{-1}.d^{-1}
170 (from the beginning to the end of the experiment). The 113 ± 1 day-old individuals
171 (days post-fertilization) at the start of the growth experiment measured on average 1.16
172 ± 0.24 mm L3. Each treatment was performed in small tanks (4 L) in triplicate (6 tanks;
173 18 polychaetes per tank; total of 108 worms). The water temperature was maintained at
174 17 ± 1°C and at a salinity of 18 ± 1 psu (temperature and salinity conditions favourable
175 to *Hediste* growth) (Olivier et al., 1996; Batista et al., 2003). The worms were reared
176 without sediment, but plastic tubes (Ø = 4 mm; several lengths) were added to provide
177 refuge to reduce stress (adapted from Nesto et al., 2018). The tanks were continuously
178 aerated to maintain oxygen concentration close to saturation for the given temperature
179 (Galasso et al., 2018). Individual wet weight was measured on days 177 and 211, and
180 individual L3 length on days 113, 144, 177 and 211. The worms were weighed
181 individually after a fasting period of 24 h to empty their digestive tract. They were then
182 carefully taken from the water using a dip net, cleaned with seawater and dried on paper
183 towels before being weighed on an analytical balance with a precision of 0.001 g.
184 Specific growth rate was calculated as $SGR = \frac{\log WW_f - \log WW_i}{t_f} \times 100$, where WW_i and
185 WW_f is the wet weight (g) at the beginning and the end of the experiment respectively,
186 and *t* is the experiment duration (d) (Hopkins, 1992). A Two-way Anova was performed
187 to test the effect of food type (fixed factor, n= 2, Fish feed and Fish faeces) and tank
188 (random factor, n=3) on WW and L3 at each biometry data. In total, 54 individuals were
189 measured per food type.

190 **2.2.3 Oxygen consumption**. The oxygen consumption rates of the ragworms were
191 recorded as a proxy of the minimal metabolic rate (the standard metabolic rate) at four
192 temperatures (11°C, 17°C, 22°C and 27°C). The oxygen consumption could be

193 considered a proxy of the minimal metabolic rate as it was measured on individuals that
194 had fasted for 24 h in the dark. A detailed description of the experiments and results are
195 presented in Galasso et al. (2018). The individuals ranged from 0.02 to 0.57 g WW, and
196 1.40 to 3.64 mm L3. The polychaetes were acclimatized for 10 days and fed *ad libitum*
197 with seabass *Dicentrarchus labrax* faeces, then acclimatized for 7 days at the
198 experimental temperature conditions. The incubation times were chosen to prevent
199 oxygen saturation from dropping below 80%. Consequently, incubation times varied
200 from 4 h (for the aquariums at 22°C and 27°C) to 5 h (for those at 11°C and 17°C). The
201 results were expressed in µmol/h.
202
203 **2.2.4 Ammonia excretion.** An ammonia excretion experiment was performed
204 simultaneously with oxygen consumption measurements. Water samples (50 mL) were
205 taken at the beginning of the experiment (t_0) (filtered seawater was used to fill the
206 individual chambers) and at the end of incubation (t_f), and immediately frozen at -20°C
207 for further ammonium analyses ($N\text{-}NH_4$). The ammonium concentrations were
208 measured using Seal AA3 analytical autoanalyser standard methods (Aminot and
209 Kérouel, 2007) with fluorometric detection (from JASCO, FP-2020plus, France).
210 Ammonia excretion rates were determined following the equation used by Galasso et al.
211 (2018) for oxygen. $N\text{-}NH_4$ was transformed to $N\text{-}NH_3$ using the conversion factor 1.22
212 (based on molar mass).

213 **2.3. Comparison between predicted and observed data**

214 Simulations were then carried out to compare the output of the model to data from
215 laboratory experiments on growth performance, oxygen consumption ($\dot{J}_O$) and ammonia

excretion ($\dot{J}_N$). In DEB theory, $\dot{J}_O$ and $\dot{J}_N$ are weighted sums of three basic fluxes: assimilation ($\dot{p}_A$), dissipation ($\dot{p}_D$) and growth ($\dot{p}_G$) (see S1 for details and equations). First, optimizations of scaled functional response (*f*) were performed to evaluate the assimilation rate of the polychaetes. This was performed using the cma_es function from the cmaes package in R (Trautman et al., 2011) run to minimize the mean relative error (MRE) between predicted and observed data. First an *f* value was obtained for the period prior to the growth experiment (until 113 days of age), and then an *f* value was fitted for each feeding condition (fish faeces or fish feed) in the growth experiment. The last L3 length was not used in the fitting process because of high size-specific mortality related to reproduction. As individuals become green at maturity (Dales, 1950), we used this criteria to remove these individuals from the group and from the dataset. Water temperatures during the different experiments were included in the model.

Second, since the oxygen consumption and ammonia excretion experiment was performed using individuals fed on faeces, the *f* fitted using the growth experiment on individuals fed faeces was used for simulating these variables. In addition, as the polychaetes used in the respiration and excretion experiment were collected in the wild, the age and life histories of these individuals were unknown. The scaling with the length and weight was therefore obtained using the DEB model run for individuals with identical life histories (but different ages). Therefore, all the observed differences in lengths within this experiment were linked to differences in age. Finally, since the experiment was performed on polychaetes that had been starved for 24 h, we assumed that the oxygen consumption and ammonia excretion associated to energy assimilation was null ($\dot{p}_A = 0$).

2.4. IMTA scenarios: temperature and assimilation rates

240 **2.4.1 Effects of temperature and assimilation rate variations**. We evaluated the
241 effects of two key factors that may affect growth: temperature and assimilation rates. As
242 temperature is the main factor in metabolism changes, especially in ectotherms (Wieser,
243 1973), the effect of a large range of temperatures from 5°C to 25°C (in 5°C increments),
244 with fixed optimal feeding conditions (scaled functional response, f=1), was tested. This
245 range was selected based on temperature variations observed in *H. diversicolor* habitats
246 (Scaps, 2002) and temperatures that are recorded in European aquaculture production
247 from Norway to Mediterranean Sea (ex. Brigolin et al. 2014; Wang et al. 2020).
248 Assimilation rates were also tested, with f ranging from 0.5 to 1 (half ration of *ad*
249 *libitum* to full *ad libitum*) (in 0.1 increments), at a constant 20°C temperature.

250 The gonadosomatic index (GSI) is the ratio between gonad mass and total body mass.
251 Using DEB theory, GSI is estimated as the ratio between the reproduction buffer wet
252 mass and the wet weight of the animal (see S1). The GSI could therefore be estimated
253 for each age in the growth experiment. In parallel, survival was recorded during the
254 growth experiment. It was assumed to be mostly related to the spawning event (and the
255 associated death) of the animals. We posited that spawning was triggered above a
256 certain GSI threshold. The survival curve was fitted over time using a sigmoid function
257 with the nls function in R (3.6.2) and Rstudio (1.2.5033). This enabled us to create a
258 link between the estimated GSI and survival. The curve was fitted with a polynomial
259 curve (of degree 5) using the poly function in R in order to obtain links between
260 survival and any GSI. Only the results from the growth experiment using faeces were
261 used for these estimations, since faeces are intended to be the most important food
262 source in a well-designed IMTA system. A GSI of 3% was chosen for the
263 bioremediation simulations since survival was high until this threshold (>90%).
264

2.4.2 Bioremediation capacity. To estimate the bioremediation capacity of polychaete to consume fish solid wastes**,** total assimilated energy was estimated over a ragworm production cycle (from birth to harvest) in several scenarios (at 20°C with *f*=0.5 or *f*=1, and at 5°C and 25°C with *f*=1). In aquaculture, a good compromise between reaching commercial weight and survival rates has to be found. For each scenario, simulations were either stopped when the GSI reached 3%, or when individual reached 0.5 g WW (minimum polychaete market size, Nesto et al. 2012). Total assimilated energy (J) was then transformed into grams of dry weight (g DW) of faeces considering that the energy content of one g (DW) of fish faeces was 10.4 kJ. We based our estimation on the average composition of seabass faeces: proteins (14%), lipids (4.6%), carbohydrates (12.8%), fibre (40.6%), and ash (28%) (Galasso et al., 2017), and the associated respective energy contents of 23.6 $kJ.g^{-1}$, 36.2 $kJ.g^{-1}$, 17.2 $kJ.g^{-1}$, 8 $kJ.g^{-1}$ and 0 $kJ.g^{-1}$ (Brigolin et al., 2014; Chary et al., 2020). Based on information provided in another study (Scaps, 2002), we considered a population density of 3700 $ind.m^{-2}$ and estimated the bioremediation capacity of a ragworm farm per m^2 for a year-round production, considering the life expectancy of the ragworms and the control of *H. diversicolor* reproduction (Wang et al., 2020).

3. Results and discussion

The results from our simulations obtained for *H. diversicolor* using DEB theory provided a good fit with new empirical data on growth, oxygen consumption and excretion in aquaculture conditions. This new empirical data set was not used for the optimization of the parameters available online (Lefebvre, 2019), and therefore we applied it in order to independently validate the parameter set.

288 **3.1 Growth rates and food quality.** The effect of the two food types, Fish faeces and
289 Fish feed, on the growth rates of *Hediste diversicolor* are presented in Table 2. After 98
290 days of the experiment, polychaetes fed with Fish faeces had a slightly (NS) higher final
291 weight (0.41 ± 0.17 g) and length (L3 = 0.30 ± 0.05 cm) than those fed with Fish feed
292 (WW= 0.36 ± 0.15 g and L3= 0.28 ± 0.06 cm). Significant difference between treatment
293 was only observed on day 177 (two-way Anova test, see Table 2). Individual growth
294 rates (from day 113 to 177) were 0.03 mm L3.d^{-1} and 5 mg WW.d^{-1} (3.8% SGR) for
295 faeces, and 0.02 mm L3.d^{-1} and 4.2 mg WW.d^{-1} (3.5% SGR) for feed. We used the DEB
296 model as an explanatory tool to estimate scaled functional response (*f*) levels in our
297 growth experiment. *f* were estimated at 0.6 and 0.5, for Fish faeces and Fish feed
298 respectively, resulting in slightly higher growth rates for *H. diversicolor* feed with Fish
299 faeces. The DEB simulation fit well with observed length data in the growth experiment
300 (Figure 2), with an MRE of 0.11. In results obtained in other studies, a high variation in
301 growth rates has been observed in relation to food quality. For example, in similar
302 conditions of temperature and salinity (25 psu, 18°C) and for comparable initial weights
303 (50 mg WW), lower growth rates (2.1 mg WW.d^{-1}, 1.8% SGR) were measured for *H.*
304 *diversicolor* fed with macroalgae (Olivier et al., 1996). Meziane and Retiere (2002)
305 obtained even lower growth rates (0.5 to 2.8 mg WW.d^{-1}, 0.3% to 1.9% SGR) for
306 ragworms fed with halophyte detritus in similar environmental conditions (15 psu,
307 21°C). However, Fidalgo e Costa et al. (2000) measured growth rates of 14 mg WW. d^{-1}
308 (5.5% SGR) feeding *H. diversicolor* with a post-larval shrimp diet (15 psu and 20°C).
309 High growth rates (6% to 12% d^{-1} SGR) were also recorded in Nesto et al. (2012), who
310 tested three different sources of food, including Larviva-Biomar® and a seaweed
311 (*Sargassum muticum*, a low-protein food) in *H. diversicolor* cultures. In fact, this last
312 study was used in the parameter estimation procedure for *H. diversicolor* (Lefebvre,

313 2019, Add-my-Pet), considering a maximal functional response for the best food source
314 (f =1). Wang et al. (2019) observed that *H. diversicolor* reared on fish feed (0.025 d^{-1}
315 SGR) grew significantly faster than worms grown on the other diets, including smolt
316 waste (0.012 d^{-1} SGR). The difference between their growth rates and the rates
317 measured in our study may originate from varying food quality and other different
318 experimental conditions, i.e. presence/absence of sediment. Indeed, in our experiment,
319 food was provided *ad libitum*, suggesting that f=1. The fitted f values of 0.5 and 0.6
320 obtained in our study probably result from a lower digestibility of fish waste compared
321 to other food sources (see Lefebvre et al., 2000). Further experiments could be
322 performed to investigate these hypotheses. Nevertheless, our results showed that despite
323 differences in food quality, growth rates were in the range of other studies. More
324 importantly, although fish waste does not lead to the best SGR compared to other
325 studies, our results indicate that it is a suitable food type for the development, growth
326 and reproduction of *H. diversicolor* in the context of IMTA.
327
328 **3.2 Suicide reproduction and GSI.** It is important to anticipate reproduction,
329 especially when it is associated to death, as is the case for semelparous species. In
330 ragworm aquaculture, harvesting would have to be performed just before reproduction
331 when worms have reached minimum market size (0.5 g WW, Nesto et al., 2012). In our
332 study, observations of the first mortalities attributed to suicide reproduction were made
333 on day 144 (mean survival of 94%). On day 211, mortality reached 43% for individuals
334 fed fish faeces and 52% for individuals fed fish feed. Using DEB simulation, we were
335 able to attribute a GSI to these individuals (Figure 3). We used a GSI of 3% as a
336 threshold for harvesting the individuals during the bioremediation simulations. Indeed,
337 under a GSI of 3%, a survival rate above 90% was estimated (Figure 3). This threshold

was estimated from our growth experiment only. Further studies in which GSI is measured on live animals are therefore needed to confirm this threshold. Environmental factors may greatly influence reproduction, including temperature and photoperiod variations (Scaps, 2002; Nesto et al., 2018). In a natural environment, Olive and Garwood (1981) observed the first appearance of developed oocytes in *H. diversicolor* coelom after 18 months. In our study, polychaetes started to reproduce after 5 months, which may indicate that aquaculture conditions with a stable temperature and stable feed input were more favourable to ragworms than natural conditions. Maturation around 4 months under control environment has been observed previously (Nesto et al., 2012). The DEB framework allows simulations to be performed in an environment in which food and temperature vary over time, and therefore estimations of *in situ* age at death (i.e. reproduction) could be performed in the wild as long as temperatures and food conditions are available.

3.3 Oxygen consumption and ammonia excretion rates. The results showed that oxygen consumption (metabolic rate) and ammonia excretion rates increased with body size (WW and L3) and temperature (Figures 4 and 5). The DEB outputs for oxygen consumption and ammonia excretion at different temperatures correctly fit observed data despite the wide variability in oxygen consumption, ranging from 0.09 to 2.35 $\mu mol.h^{-1}$ (Figure 4) (Galasso et al., 2018), and ammonia excretion, ranging from 4.10^{-6} to 0.58 $\mu mol.h^{-1}$ (Figure 5). The fit between the oxygen consumption data and the predictions was better than for the ammonia excretion data, with respective MREs of 0.51 and 0.80. It appeared that the ammonia results were underestimated by the model. The ammonia results were more scattered than the oxygen consumption rate results. The incubation times was short to keep a good oxygen saturation and concentrations were

363 close to the detection limit. A longer incubation period and no previous starvation may
364 have provided less variable data. In marine species, an increase in ammonia excretion
365 with increased temperature is well known, including for invertebrates (Chen and Lai,
366 1993). In contrast to fish, very little is known regarding the ammonia excretion
367 mechanism and the participating excretory organs in marine invertebrates, especially in
368 polychaetes (Thiel et al., 2017). Thus, our study provides valuable data on this topic,
369 which will need further quantitative data in order to properly characterize nutrient fluxes
370 in IMTAs.
371
372 **3.4 Bioremediation potential.** We found that growth rates increased with increasing
373 temperatures (Figure 6) and scaled functional response (*f*, Figure 7). For the
374 bioremediation estimation, simulations were stopped when GSI reached 3% or 0.5 g
375 WW, considered as the minimum market size. The results from selected scenarios are
376 shown in Table 3. At 20°C, an increased assimilation rate (higher *f*) reduced the time to
377 reach the GSI threshold (99 days with *f*=0.5 vs 79 days with *f*=1). At this stage,
378 ragworms weighed only 0.2 g at *f*=0.5 compared to 0.6 g when *f*=1. At the maximum
379 assimilation rate (*f*=1), increased temperature (5°C vs 25°C) decreased the time to reach
380 a GSI of 3% (163 days at 5°C vs 64 days at 25°C), but had no effect on the final wet
381 weight (0.6 g). Similar observations were made when simulations were stopped at a wet
382 weight of 0.5 g. It should be noted that at 20°C with *f*=0.5, the minimum market size of
383 0.5 g was reached in 128 days, but with a GSI of 3.9%. In a bioremediation perspective,
384 the potential of *H. diversicolor* was estimated based on cumulated assimilation rates
385 ($\dot{p}_A$). Assuming an energy content of 10.4 $kJ.g^{-1}$ DW of seabass faeces, and based on the
386 high density of *H. diversicolor* (3700 ind. m^{-2}) reported in nature (Scaps, 2002), we
387 estimated a bioremediation capacity ranging from 0.23 to 0.87 g faeces DW ind^{-1} $year^{-1}$,

388 eq of 755 to 2887 g faeces DW m^{-2} $year^{-1}$ (Table 3). This could represent 75-289 kg for
389 a 100 m^2 ragworm farm, equivalent to a 2-9 % reduction in the waste produced by a
390 20T seabass farm (160 kg of DW faeces per ton of seabass production, based on
391 assimilation coefficients in Brigolin et al., 2014). This study therefore confirms the
392 potential of *H. diversicolor* in IMTA systems, in particular associated with fish farms,
393 as has been shown in previous studies (Batista et al., 2003; Bischoff et al., 2009; Cubillo
394 et al., 2016 and Marques et al., 2017). Comparisons of bioremediation capacity to other
395 studies are, however, difficult as most of previous studies are site specific or based on
396 specific scenario. The quantity of faeces produced by a marine fish farms depends on
397 numerous factors (species, conversion ratio, temperature, farm management, etc) and
398 can vary from 160 kg of DW faeces per ton of seabass production (Brigolin et al., 2014)
399 to 224 Kg of DW faeces per ton of salmon production (see review by van Rijn, 2013).
400 Wang et al. (2019) estimated that 1 Kg of fish released 250 g of faeces and 30 g of
401 uneaten feed and could produce 800 g of *H. diversicolor*. Considering the feed
402 conversion ratio (g dry faeces used/g polychaete biomass produced) of 3.55 given by
403 the authors, we could estimate a bioremediation capacity of 23 g of fish faeces, eq 9.2 %
404 of faeces reduction (ragworm density was not provided in this study). Chary et al.
405 (2020) compared studies using mathematical models to examine uptake of solid organic
406 matter or nutrients in IMTA systems by other detritivores. Conclusions were quite
407 contrasted (Chary et al., 2020). Cubillo et al. (2016) and Ren et al. (2012) predicted that
408 bottom culture of sea cucumbers could remove more than 70% of the benthic particulate
409 organic carbon (C) from Atlantic salmon (*Salmo salar*) farm units. These two studies
410 did not consider rearing constraints (limit of density) for the extractive species.
411 Including such considerations in models can help predict more realistic production
412 design and bioremediation potentials from extractive species. When considering current

density rearing practices, Watanabe et al. (2015) calculated that 4.3% of total particulate nitrogen from milkfish (*Chanos chanos*) culture could be removed by seacumber detritivore species. In the present study, the bioremediation potential was expressed per individual and per m^{-2}, and for a large range of temperature, to allow future comparisons. The DEB model allows simulations to be performed that may be useful to predict life history traits in different environmental conditions, as well as to anticipate harvest before reproduction.

Conclusion. Our results suggest that fish waste could constitute the exclusive source of food for the polychaete *Hediste diversicolor*. We were able to obtain these results using a DEB model that accurately predicted the species' metabolic processes. Further studies could build on these results by including certain environmental factors, such as water salinity, photoperiod, as well as other water temperature variations that may trigger reproduction. These findings suggest that DEB modelling is a promising tool for IMTA development. The method could help fish producers manage the use of *H. diversicolor* to complement their primary production and could also assist environmental policy by utilizing the bioremediation potential of *H. diversicolor* when associated to fish production.

Acknowledgements

The authors would like to thank Luca Florean, Osvaldo Makowiecky and Alexandre Dousset for their valuable help reviewing life history traits and in the laboratory, Thibault Geoffroy and Sébastien Triplet for their participation in the experimental work, and Marion Richard for her great help planning and conducting the oxygen consumption experiments. We thank two anonymous reviewers for their constructive comments, which helped us to improve the manuscript. We also thank Elise Bradbury for careful revision of the English. The study was carried out within the framework of

438 the ERA-Net COFASP (Strengthening Cooperation in European Research on
439 Sustainable Exploitation of Marine Resources in Seafood Chains) project (IMTA-Effect
440 project) with funding from the French National Research Agency (ANR-15-COFA-
441 0001-06). It was also supported by the Brazilian government's 'Science Without
442 Borders' programme (CAPES PhD scholarship n°13.773-13-5 awarded to HG) and the
443 European Maritime and Fisheries Fund (EPURVAL2 project) (postdoctoral grant
444 awarded to BS).

4. References

Abreu, M.H., Pereira, R., Yarish, C., Buschmann, A.H., Sousa-Pinto, I., 2011. IMTA with *Gracilaria vermiculophylla*: Productivity and nutrient removal performance of the seaweed in a land-based pilot scale system. Aquaculture 312, 77–87. doi:10.1016/j.aquaculture.2010.12.036

Aminot, A., Kérouel, R., 2007. Dosage automatique des nutriments dans les eaux marines.

Batista, F.M., Fidalgo e Costa, P., Ramos, A., Passos, A.M., Pousão Ferreira, P., Cancela da Fonseca, L., 2003. Production of the ragworm *Nereis diversicolor* (O. F. Müller, 1776), fed with a diet for gilthead seabream *Sparus auratus* L., 1758: survival, growth, feed utilization and oogenesis. Inst. Español Oceanogr. 19, 447–451.

Bischoff, A.A., Fink, P., Waller, U., 2009. The fatty acid composition of *Nereis diversicolor* cultured in an integrated recirculated system: Possible implications for aquaculture. Aquaculture 296, 271–276. doi:10.1016/j.aquaculture.2009.09.002

Brett, J.R., Groves, T.D.D., 1979. Physiological Energetics. Vol. VIII- Bioenergetics and Growth, in: Hoar W.S., Randall, D.J., Brett, J.R. (Eds.), Fish Physiology. Academic Press, London, pp. 288–344.

Brigolin, D., Pastres, R., Tomassetti, P., Porrello, S., 2010. Modelling the biomass yield and the impact of seabream mariculture in the Adriatic and Tyrrhenian Seas (Italy). Aquac. Int. 18, 149–163. https://doi.org/10.1007/s10499-008-9232-4

Brigolin, D., Meccia, V. L., Venier, C., Tomassetti, P., Porrello, S.,Pastres, R., 2014. Modelling biogeochemical fluxes across a Mediterranean fish cage farm. Aquaculture Environment Interactions 5(1): 71-88.

Cammen, L.M., 1980. The significance of microbial carbon in the nutrition of the deposit feeding Polychaete *Nereis succinea*. Mar. Biol. 61, 9–20.

Chary, K., Aubin, J., Sadoul, B., Fiandrino, A., Covès, D., Callier, M. D., 2020. Integrated multi-trophic aquaculture of red drum (*Sciaenops ocellatus*) and sea cucumber (*Holothuria scabra*): Assessing bioremediation and life-cycle impacts. Aquaculture, 516. 734621 (17p.). doi.org/10.1016/j.aquaculture.2019.734621

Chen, J.-C., Lai, S.-H., 1993. Effects of temperature and salinity on oxygen consumption and ammonia excretion of juvenile *Penaeus japonicus* Bate. J. Exp. Mar. Bio. Ecol. 165, 161–170589. doi:10.1007/s10499-008-9169-7

Chopin, T., Cooper, J.A., Reid, G., Cross, S., Moore, C., 2012. Open-water integrated multi-trophic aquaculture: environmental biomitigation and economic diversification of fed aquaculture by extractive aquaculture. Rev. Aquac. 4, 209–220. doi:10.1111/j.1753-5131.2012.01074.x

Cook, E.J., Kelly, M.S., 2007. Enhanced production of the sea urchin *Paracentrotus lividus* in integrated open-water cultivation with Atlantic salmon *Salmo salar*. Aquaculture 273, 573–585. doi:10.1016/j.aquaculture.2007.10.038

Cubillo, A.M., Ferreira, J.G., Robinson, S.M.C.C., Pearce, C.M., Corner, R.A., Johansen, J., 2016. Role of deposit feeders in integrated multi-trophic aquaculture - A model analysis. Aquaculture 453, 54–66. doi:10.1016/j.aquaculture.2015.11.031

De Cubber, L., Lefebvre, S., Lancelot, T., Denis, L., & Gaudron, S. M., 2019. Annelid polychaetes experience metabolic acceleration as other Lophotrochozoans: Inferences on the life cycle of *Arenicola marina* with a Dynamic Energy Budget model. Ecological Modelling, 411. doi.org/10.1016/j.ecolmodel.2019.108773

Erler, D. V, Pollard, P.C., Burke, M., Knibb, W., 2000. Biological remediation of aquaculture waste: a combined finfish, artificial substrate treatment system, in: Proceedings of the National Workshop of Wastewater Treatment and Integrated Aquaculture. pp. 93–107.

Fang, J., Jiang, Z., Jansen, H.M., H U, F., Fang, J., Liu, Y., Gao, Y., Du, M., 2017. Applicability of *Perinereis aibuhitensis* Grube for fish waste removal from fish cages in Sanggou Bay, P. R. China. Ocean. Coast. Sea Res. 16, 294–304. doi:10.1007/s11802-017-3256-1

Fidalgo e Costa, P., Narciso, L., Fonseca, L.C., 2000. Growth, survival and fatty acid profile of *Nereis diversicolor* (O. F. Müller, 1776) fed on six different diets. Bulletin of Marine Science, 67(1): 337–343.

Filgueira, R., Guyondet, T., Reid, G.K., Grant, J., Cranford, P.J., 2017. Vertical particle fluxes dominate integrated multi-trophic aquaculture (IMTA) sites: implications for shellfish – finfish synergy 9, 127–143.

Galasso, H.L., Callier, M. D., Bastianelli, D., Blancheton, J.-P., & Aliaume, C., 2017. The potential of near infrared spectroscopy (NIRS) to measure the chemical composition of aquaculture solid waste. Aquaculture, 476. https://doi.org/10.1016/j.aquaculture.2017.02.035

Galasso, Helena Lopes, Richard, M., Lefebvre, S., Aliaume, C., & Callier, M. D., 2018. Body size and temperature effects on standard metabolic rate for determining metabolic scope for activity of the polychaete *Hediste* (*Nereis*) *diversicolor*. PeerJ, 6. https://doi.org/10.7717/peerj.5675

Gillet, P., Mouloud, M., Durou, C., Deutsch, B., 2008. Response of *Nereis diversicolor* population (Polychaeta, Nereididae) to the pollution impact – Authie and Seine estuaries (France). Estuar. Coast. Shelf Sci. 76, 201–210. doi:10.1016/j.ecss.2007.07.004

Hargrave, B.T. (Ed.), 2005. Environmental Effects of Marine Finfish Aquaculture, Handbook of Environmental Chemistry. Springer-Verlag, Berlin/Heidelberg. https://doi.org/10.1007/b12227

Hedman, J.E., Gunnarsson, J.S., Samuelsson, G., Gilbert, F., 2011. Particle reworking and solute transport by the sediment-living polychaetes *Marenzelleria neglecta* and *Hediste diversicolor*. J. Exp. Mar. Bio. Ecol. 407, 294–301. doi:10.1016/j.jembe.2011.06.026

Heilskov, A.C.C., Holmer, M., 2001. Effects of benthic fauna on organic matter mineralization in fish-farm sediments: importance of size and abundance. ICES J. Mar. Sci. 58, 427–434. doi:10.1006/jmsc.2000.1026

Hopkins, K.D., 1992. Reporting Fish Growth: A Review of the Basics. Journal of the World Aquaculture Society. 23, 173-179

Jansen, H. M., Broch, O. J., Bannister, R., Cranford, P., Handa, A., Husa, V., Jiang, Z., Strohmeier, T.,Strand, O., 2018. Spatio-temporal dynamics in the dissolved nutrient waste plume from Norwegian salmon cage aquaculture. Aquaculture Environment Interactions 10: 385-399.

Jiang, Z., Wang, G., Fang, J., Mao, Y., Bay, A., 2013. Growth and food sources of Pacific oyster *Crassostrea gigas* integrated culture with Sea bass Lateolabrax. Aquac. Int. 21, 45–52. doi:10.1007/s10499-012-9531-7

Kooijman, S. (2010). Dynamic Energy Budget theory for metabolic organisation. Cambridge Univ. Press, Cambridge

Kooijman, S.A.L.M, Pecquerie L., Augustine S, Jusup, M., 2011. Scenarios for acceleration in fish development and the role of metamorphosis. Journal of Sea Research. 66, 4, 419–423

545 Katz, T., Herut, B., Genin, A., Angel, D.L., 2002. Gray mullets ameliorate organically
546 enriched sediments below a fish farm in the oligotrophic Gulf of Aqaba (Red
547 Sea). Mar. Ecol. Prog. Ser. 234, 205–214. doi:10.3354/meps234205
548 Kristensen, E., 1983. Ventilation and oxygen uptake by three species of *Nereis*
549 (Annelida: Polychaeta). II. Effects of temperature and salinity changes. Mar.
550 Ecol. Prog. Ser. 12, 299–306.
551 Lefebvre, S., Barille, L., Clerc, M., 2000. Pacific oyster (*Crassostrea gigas*) feeding
552 responses to a fish-farm effluent. Aquaculture 187(1-2): 185-198.
553 Lefebvre, S., 2019. AmP *Hediste diversicolor*, version 2019/09/28
554 MacDonald, C.L.E., Stead, S.M., Slater, M.J., 2013. Consumption and remediation of
555 European Seabass (*Dicentrarchus labrax*) waste by the sea cucumber *Holothuria*
556 *forskali*. Aquac. Int. 21, 1279–1290. doi:10.1007/s10499-013-9629-6
557 Marques, B., Calado, R., Lillebø, A.I., 2017. New species for the biomitigation of a
558 super-intensive marine fish farm effluent: Combined use of polychaete-assisted
559 sand filters and halophyte aquaponics. Sci. Total Environ. 599–600, 1922–1928.
560 doi:10.1016/j.scitotenv.2017.05.121
561 Mermillod-Blondin, F., Rosenberg, R., François-Carcaillet, F., Norling, K., Mauclaire,
562 L., 2004. Influence of bioturbation by three benthic infaunal species on
563 microbial communities and biogeochemical processes in marine sediment.
564 Aquat. Microb. Ecol. 36, 271–284. doi:10.3354/ame036271
565 Meziane, T., Retiere, C., 2002. Growth of *Nereis diversicolor* (L.) juveniles fed with
566 detritus of halophytes. Oceanol. Acta 25, 119–124.
567 Michaud, E., Desrosiers, G., Mermillod-Blondin, F., Bjorn Sundby, Georges Stora,
568 2006. The functional group approach to bioturbation: II. The effects of the
569 *Macoma balthica* community on fluxes of nutrients and dissolved organic
570 carbon across the sediment–water interface. Journal of Experimental Marine
571 Biology and Ecology, 337, Issue 2, 178-189
572 Nelson, E.J., MacDonald, B. a. A., Robinson, S.M.C., 2012. The absorption efficiency
573 of the suspension-feeding sea cucumber, *Cucumaria frondosa*, and its potential
574 as an extractive integrated multi-trophic aquaculture (IMTA) species.
575 Aquaculture 370–371, 19–25. doi:10.1016/j.aquaculture.2012.09.029
576 Nesto, N., Simonini, R., Prevedelli, D., Da, L., 2018. Evaluation of different procedures
577 for fertilization and larvae production in *Hediste diversicolor* (O. F. Müller,
578 1776) doi:10.1111/are.13589
579 Nesto, N., Simonini, R., Prevedelli, D., Ros, L. Da, 2012. Effects of diet and density on
580 growth, survival and gametogenesis of *Hediste diversicolor* (O. F. Müller, 1776)
581 (Nereididae, Polychaeta). Aquaculture 362–363, 1–9.
582 doi:10.1016/j.aquaculture.2012.07.025
583 Neori, A., Chopin, T., Troell, M., Buschmann, A.H., Kraemer, G.P., Halling, C.,
584 Shpigel, M., Yarish, C., 2004. Integrated aquaculture: rationale, evolution and
585 state of the art emphasizing seaweed biofiltration in modern mariculture.
586 Aquaculture 231, 361–391.
587 doi:http://dx.doi.org/10.1016/j.aquaculture.2003.11.015
588 Nielsen, A.M., Eriksen, N.T., Iversen, J.J.L., Riisgård, H.U., 1995. Feeding, growth and
589 respiration in the polychaetes *Nereis diversicolor* (facultative filter feeder) and
590 *N. virens* (omnivorous) - a comparative study. Mar. Ecol. Prog. Ser. 125, 149–
591 158. doi:10.3354/meps125149
592 Olive, P.J.W., Garwood, P.R.G., 1981. Gametogenic cycle and population structure of
593 *Nereis (Hediste) diversicolor* and *Nereis (Nereis) pelagica* from north-east
594 England. J. Maine Biol. Ass 61, 193–213.

595 Olivier, M., Desrosiers, G., Caron, A., Ret, 1996. Juvenile growth of the polychaete
596 *Nereis virens* feeding on a range of marine vascular and macroalgal plant
597 sources. Marine 125, 693–699.
598 Orr, L.C., Curtis, D.L., Cross, S.F., Gurney-Smith, H., Shanks, A., Pearce, C.M., 2014.
599 Ingestion rate, absorption efficiency, oxygen consumption, and fecal production
600 in green sea urchins (*Strongylocentrotus droebachiensis*) fed waste from
601 sablefish (*Anoplopoma fimbria*) culture. Aquaculture 422–423, 184–192.
602 doi:10.1016/j.aquaculture.2013.11.030
603 Ozoh, P.T.E., Jones, N. V, 1990. The effects of salinity and temperature on the toxicity
604 of copper to 1-day and 7-day-old larvae of *Hediste (Nereis) diversicolor* (O. F.
605 Müller). Ecotoxicol. Environ. Saf. 19, 24–32. doi:10.1016/0147-6513(90)90075-
606 G
607 Paltzat, D.L., Pearce, C.M., Barnes, P. a. A., McKinley, R.S., 2008. Growth and
608 production of California sea cucumbers (*Parastichopus californicus Stimpson*)
609 co-cultured with suspended Pacific oysters (*Crassostrea gigas* Thunberg).
610 Aquaculture 275, 124–137. doi:10.1016/j.aquaculture.2007.12.014
611 Papaspyrou, S., Thessalou-Legaki, M., Kristensen, E., 2010. The influence of infaunal
612 (*Nereis diversicolor*) abundance on degradation of organic matter in sandy
613 sediments. J. Exp. Mar. Bio. Ecol. 393, 148–157.
614 doi:10.1016/j.jembe.2010.07.015
615 Porter, C.B., Krost, P., Gordin, H., Angel, D.L., 1996. Preliminary assessment of grey
616 mullet (*Mugil cephalus*) as a forager of organically enriched sediments below
617 marine fish farms. Isr. J. Aquac. Bamidgeh 48, 47–55.
618 Ren, J. S., Stenton-Dozey, J., Plew, D. R., Fang, J., & Gall, M., 2012. An ecosystem
619 model for optimising production in integrated multitrophic aquaculture systems.
620 Ecological Modelling, 246, 34–46. doi.org/10.1016/j.ecolmodel.2012.07.020
621 van Rijn, J. (2013). Waste treatment in recirculating aquaculture systems. Aquacultural
622 Engineering 53: 49-56.
623 Reid, G.K., Lefebvre, S., Filgueira, R., Robinson, S.M.C., Broch, O.J., Dumas A.,
624 Chopin, T.B.R., 2020. Performance measures and models for open-water
625 integrated multi-trophic aquaculture. Reviews in Aquaculture 12 (1), 47-75
626 Riisgård, H.U., 1994. Filter-feeding in the polychaete *Nereis diversicolor*: a review.
627 Netherlands J. Aquat. Ecol. 28, 453–458. doi:10.1007/BF02334216
628 Scaps, P., 2002. A review of the biology, ecology and potential use of the common
629 ragworm *Hediste diversicolor* (O. F. Müller) (Annelida: Polychaeta).
630 Hydrobiologia 470, 203–218. doi:10.1023/A:1015681605656
631 Trautmann, H., Mersmann, O., Arnu, D., 2011. cmaes: Covariance Matrix Adapting
632 Evolutionary Strategy. R package version 1.0-11. https://CRAN.R-
633 project.org/package=cmaes
634 Wang, H. Q., Seekamp, I., Malzahn, A., Hagemann, A., Carvajal, A. K., Slizyte, R.,
635 Standal, I. B., Handa, A., Reitan, K. I., 2019. Growth and nutritional
636 composition of the polychaete *Hediste diversicolor* (OF Muller, 1776) cultivated
637 on waste from land-based salmon smolt aquaculture. Aquaculture 502:232–241.
638 Wang, H. Q., Hagemann, A., Reitan, K. I., Handa, A., Uhre, M., Malzahn, A. M., 2020.
639 Embryonic and larval development in the semelparous Nereid polychaete
640 *Hediste diversicolor* (OF Muller, 1776) in Norway: Challenges and perspectives.
641 Aquaculture Research 00:1–17.
642 Watanabe, S., Kodama, M., Orozco, Z.G.A., Sumbing, J.G., Novilla, S.R.M., Lebata-
643 Ramos, M.J.H., 2015. Estimation of energy budget of sea cucumber, *Holothuria*
644 *scabra*, in integrated multi-trophic aquaculture., in: M. R. R. Romana-Eguia, F.

645 D. Parado-Estepa, N. D. Salayo, & M. J. H. Lebata-Ramos (Eds.), Resource
646 Enhancement and Sustainable Aquaculture Practices in Southeast Asia:
647 Challenges in Responsible Production of Aquatic Species: Proceedings of the
648 Internation. Tigbauan, Iloilo, Philippines Aquaculture Department, Southeast
649 Asian Fisheries Development Center, pp. 307–308
650 Wieser, W., 1973. Effects of Temperature on Ectothermic Organisms: Ecological
651 Implications and Mechanisms of Compensation, 1st ed. Springer-Verlag, New
652 York Heidelberg Berlin 1973.
653

Figure 1. DEB representation of allocation rule (κ rule) and energy fluxes in an organism. Ingested energy is either assimilated or lost by defecation. Then part of the energy mobilized from the reserve (κ) is allocated for somatic maintenance and growth, and the remaining energy is spent for maturity and its associated maintenance. Once sexual maturity is reached, the energy available for maturity is used for the production of gametes (modified from Kooijman, 2010).

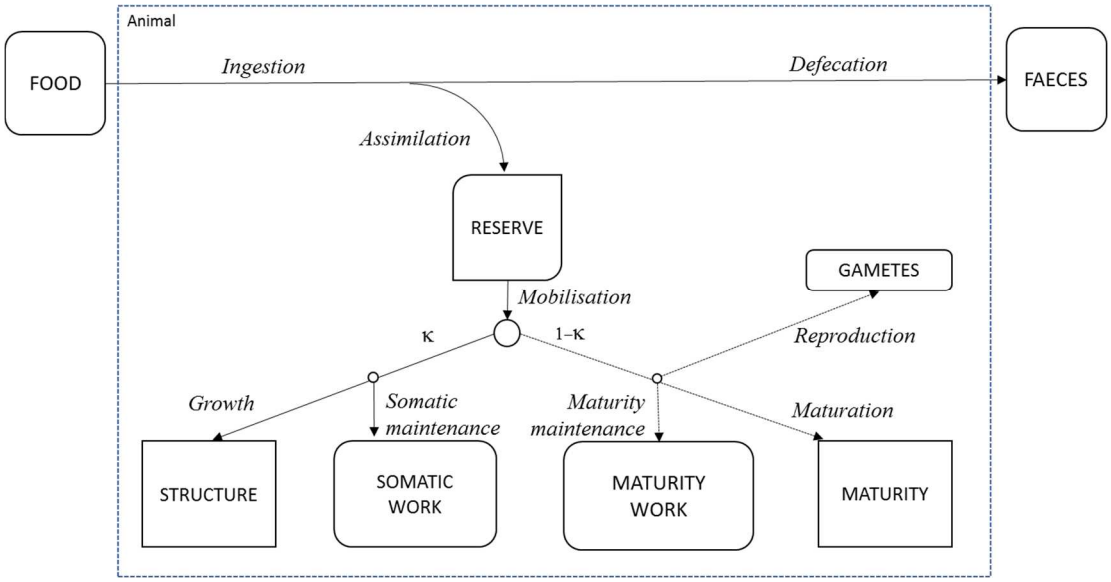

Figure 2. *Hediste diversicolor*. Comparison of DEB simulation (line) and growth data (a) L3 length (cm) and (b) wet weight (WW) (g) for polychaetes fed with Fish faeces and Fish feed. After optimization, f=0.5 for Fish feed and f=0.6 for Fish faeces. Before the experiment (dashed line), f was estimated to be 0.4. Individual WW was measured on days 177 and 211, and individual L3 length on days 113, 144, 177 and 211. The values obtained during the last biometry (211 days post-fertilization) were not included in the optimization due to high suicide reproduction. MRE = 0.11 for L3 length values.

a)

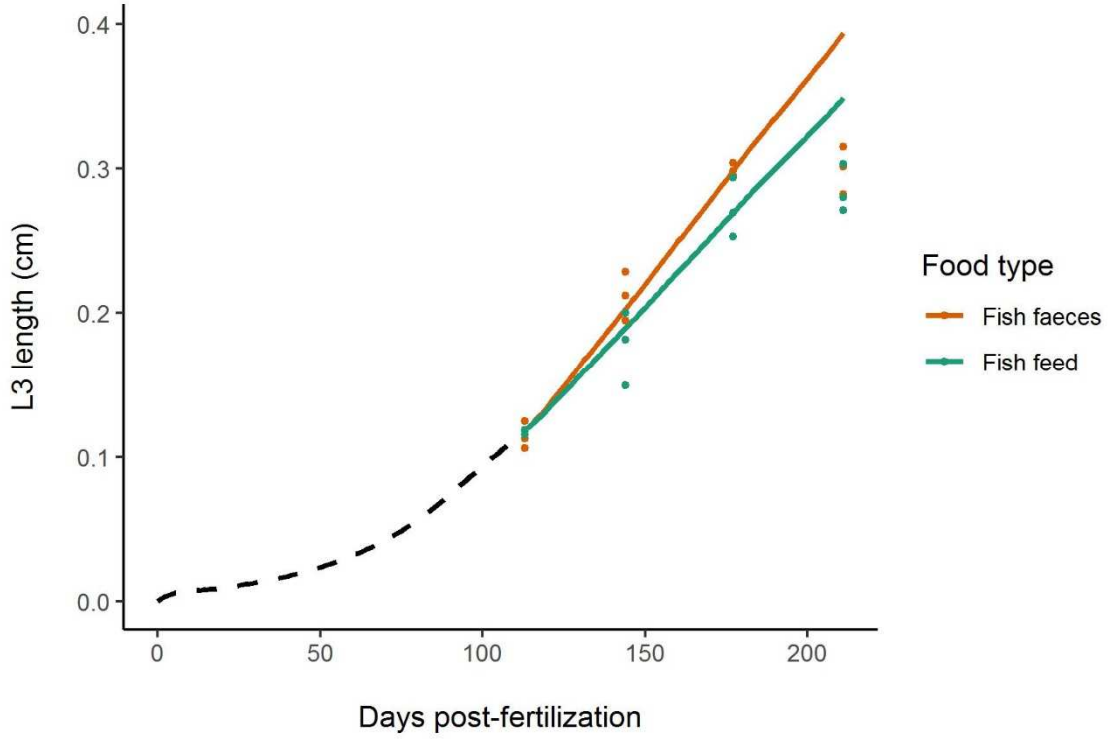

b)

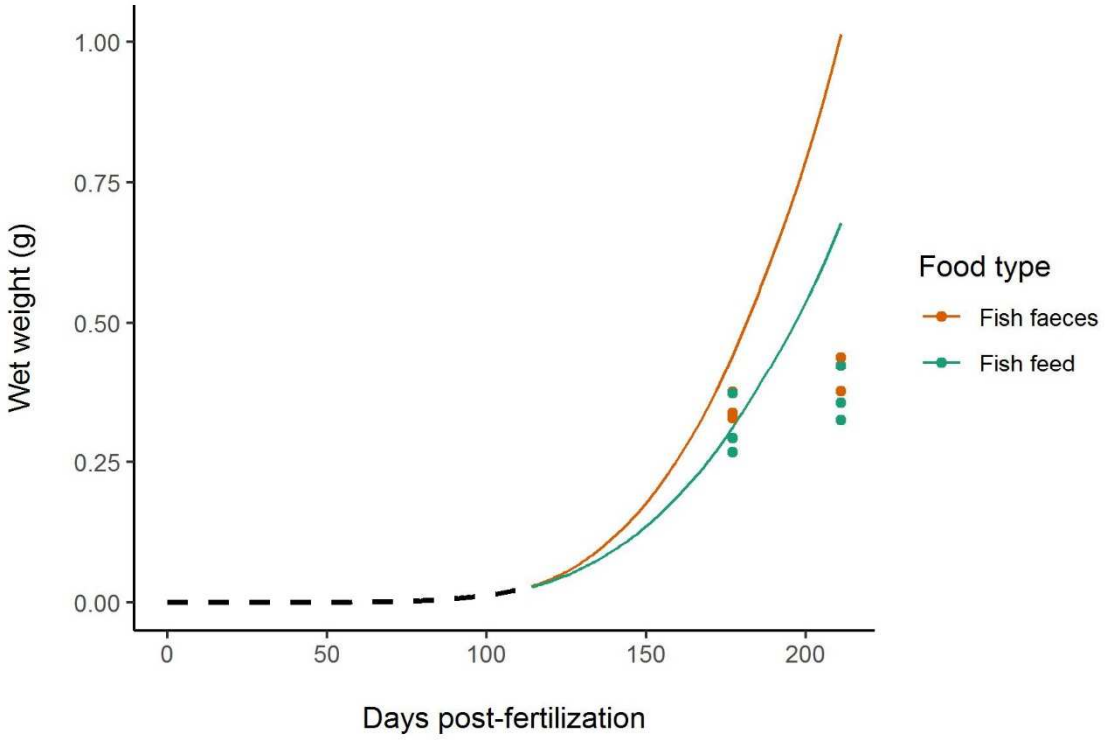
1.00
0.75
0.50
0.25
0.00
Wet weight (g)
0
50
100
150
200
Days post-fertilization
Food type
Fish faeces
Fish feed

675
676

Figure 3. Survival over time and by GSI in polychaetes fed with fish faeces. (a) Survival over time. The curve was fitted using a sigmoid (red line, $R^2 = 0.87$). (b) Survival by estimated GSI from the DEB model on ages ranging from 0 to 500 days post-fertilization. A polynomial function of degree 5 was fitted (red line, $R^2 = 1$).

a)

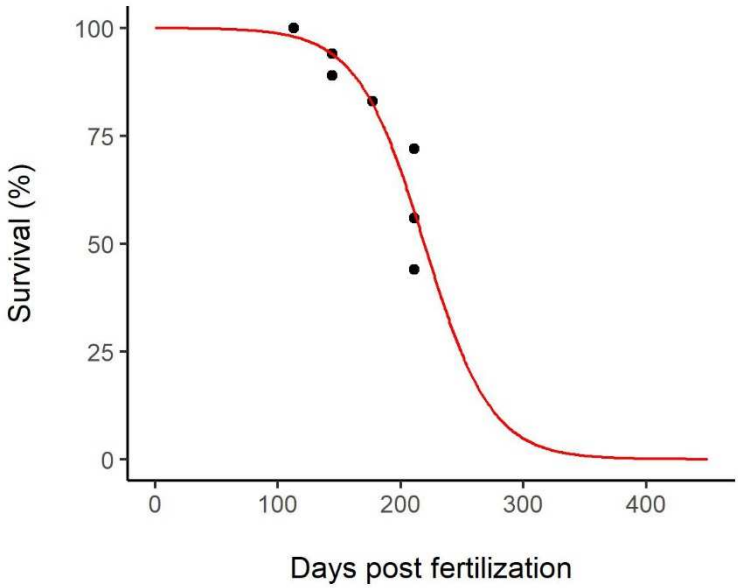

b)

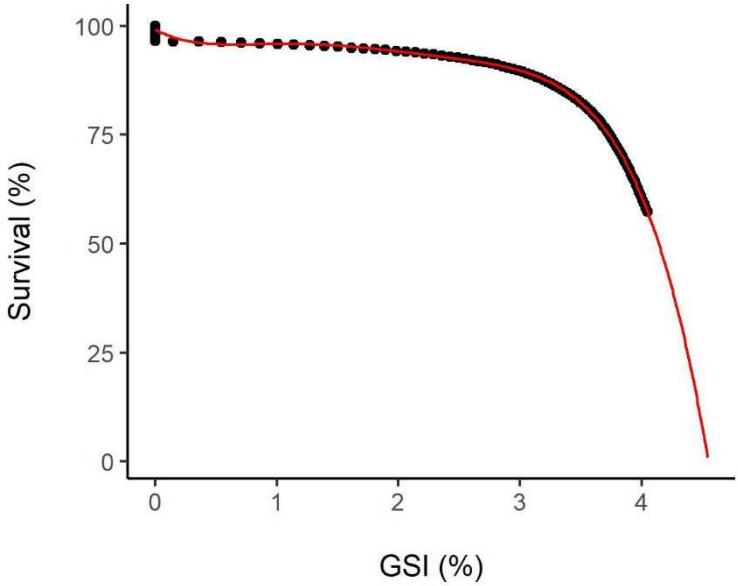

Figure 4. *Hediste diversicolor*. Comparison of DEB simulation (line) and oxygen consumption rates at four temperatures (11°C, 17°C, 22°C and 27°C) expressed over (a) L3 length (cm) and (b) wet weight (WW) (g) for polychaetes fed with fish faeces (*f* =0.6). MRE = 0.51 for L3 length and WW values.

a)

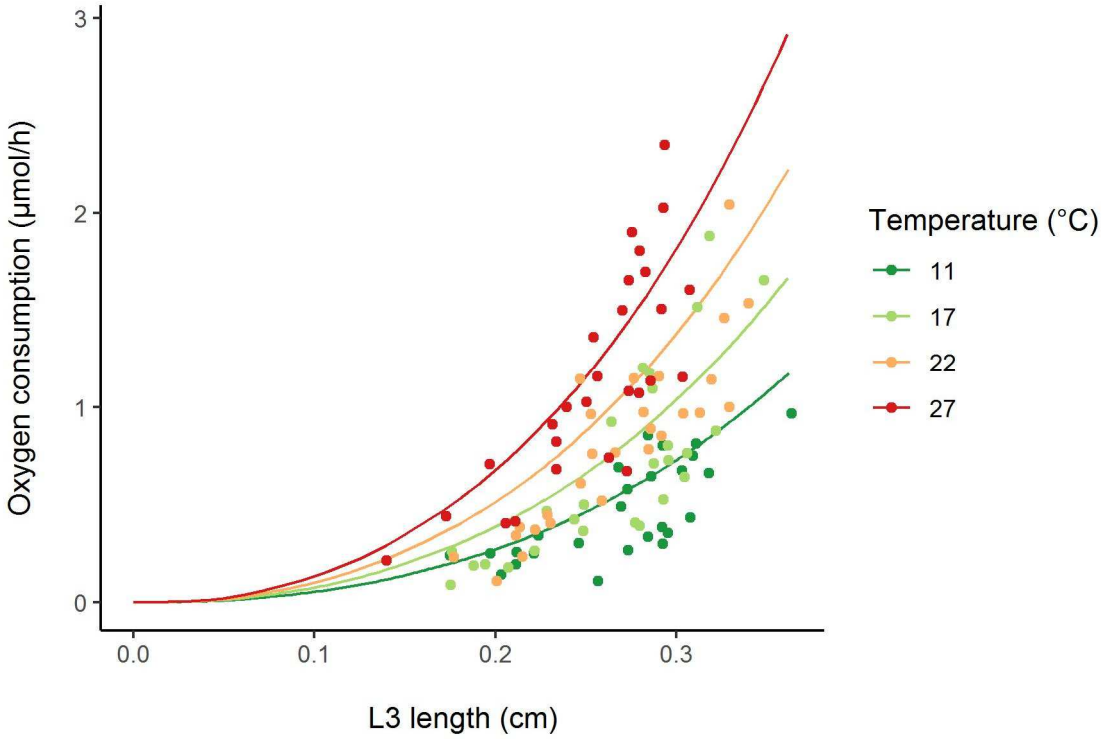

b)

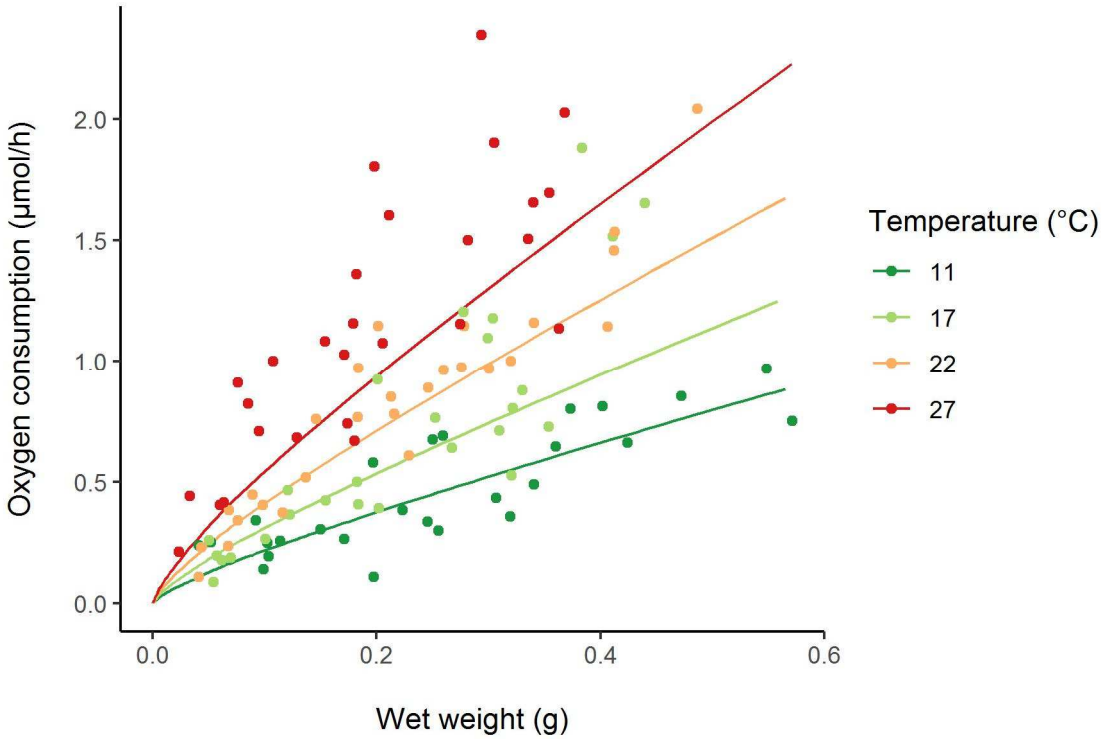

Figure 5. *Hediste diversicolor*. Comparison of DEB simulation (line) and ammonia excretion rates at four temperatures (11°C, 17°C, 22°C and 27°C) expressed over (a) L3 length (cm) and (b) wet weight (WW) (g) for polychaetes fed with fish faeces (f =0.6). MRE = 0.8 for L3 length and WW values.

a)

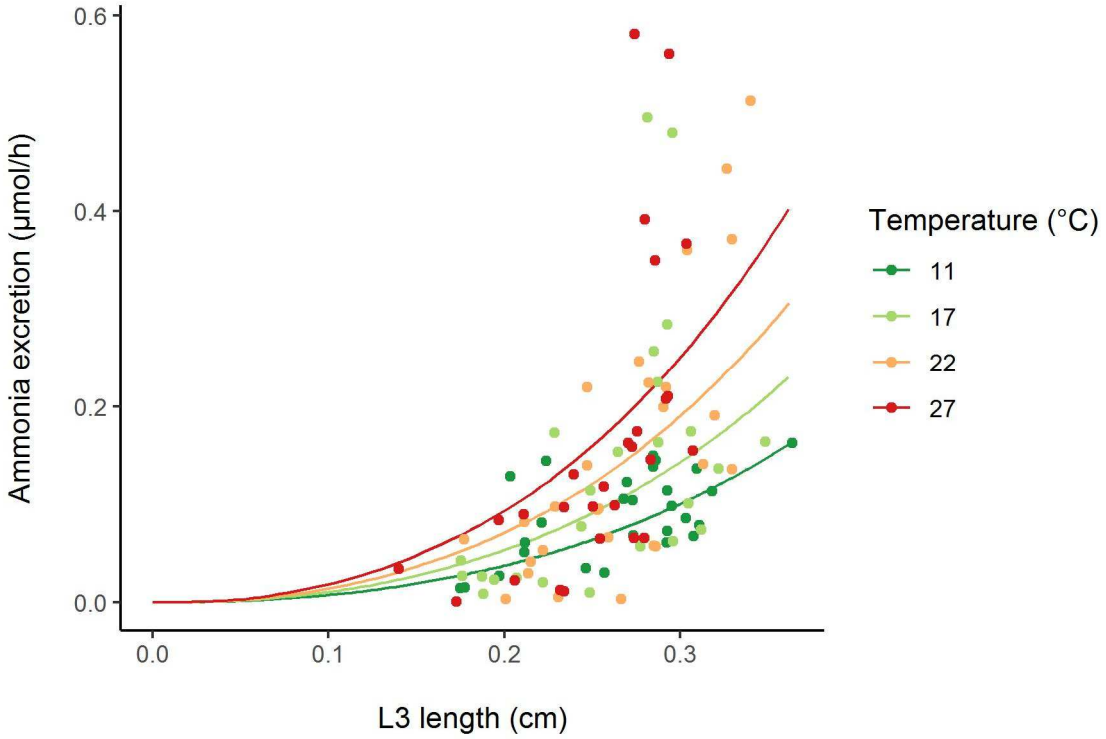

b)

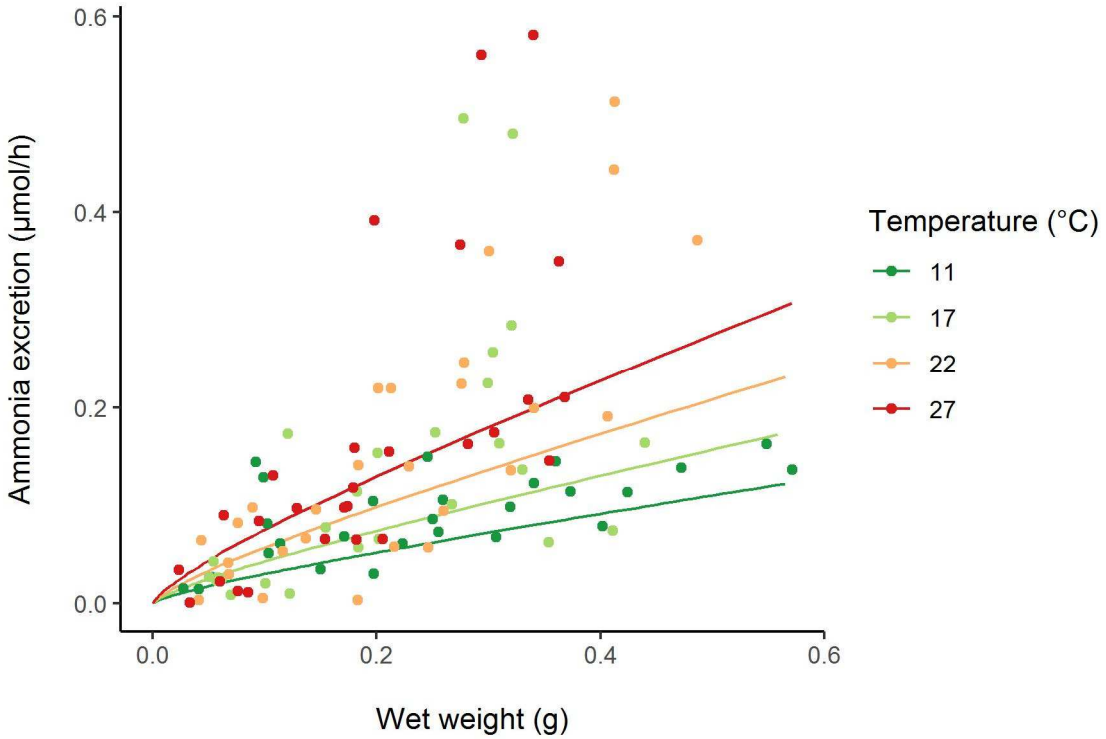

Figure 6. DEB simulations of *H. diversicolor* individual growth in L3 length (cm) and wet weight (WW) (g) with temperatures ranging from 5°C to 25°C. Simulations were performed until the maximum observed size (1.57 g, Add my Pet database, Lefebvre, 2019) (based on the literature) was reached. The functional scaled response was maintained constant at *f*=1.

a)

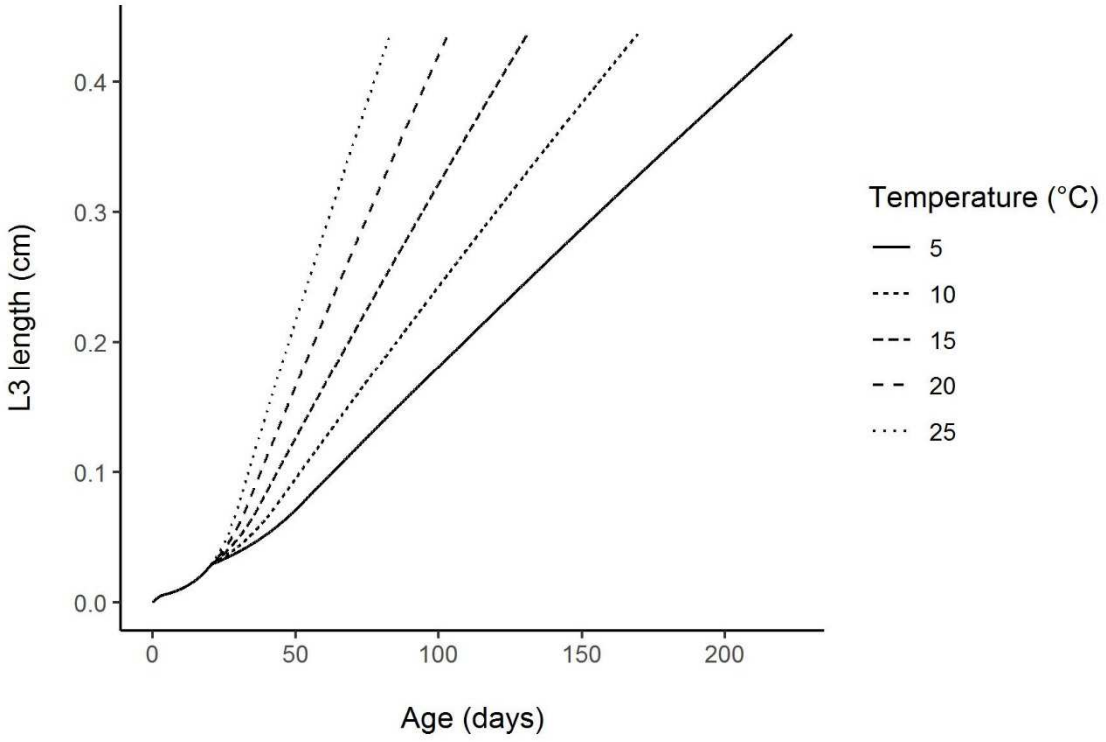

b)

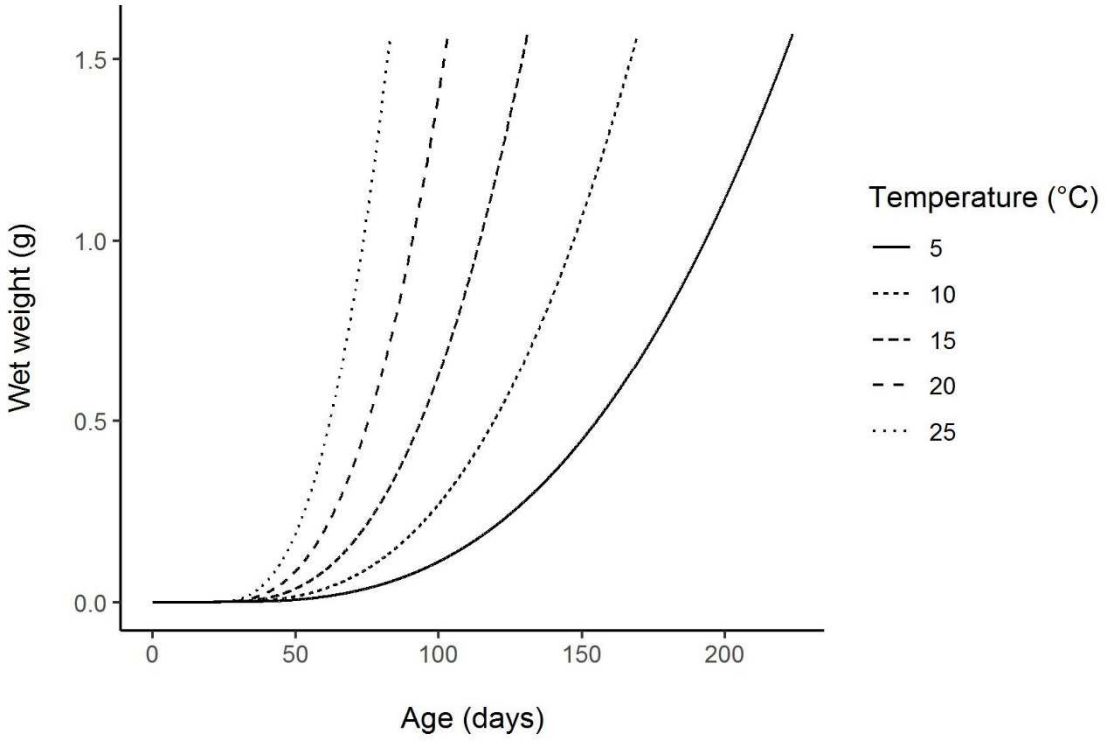

Figure 7. DEB simulations of *H. diversicolor* individual growth in a) L3 length (cm) and b) wet weight (WW) (g) over time (days) according to different food abundance (scaled functional response, *f*) scenarios. Simulations were performed until the GSI for first reproduction was reached (3%). The temperature was maintained constant at 20°C. *f* at 0.5 means that individuals were fed at 50% of *ad libitum*.

a)

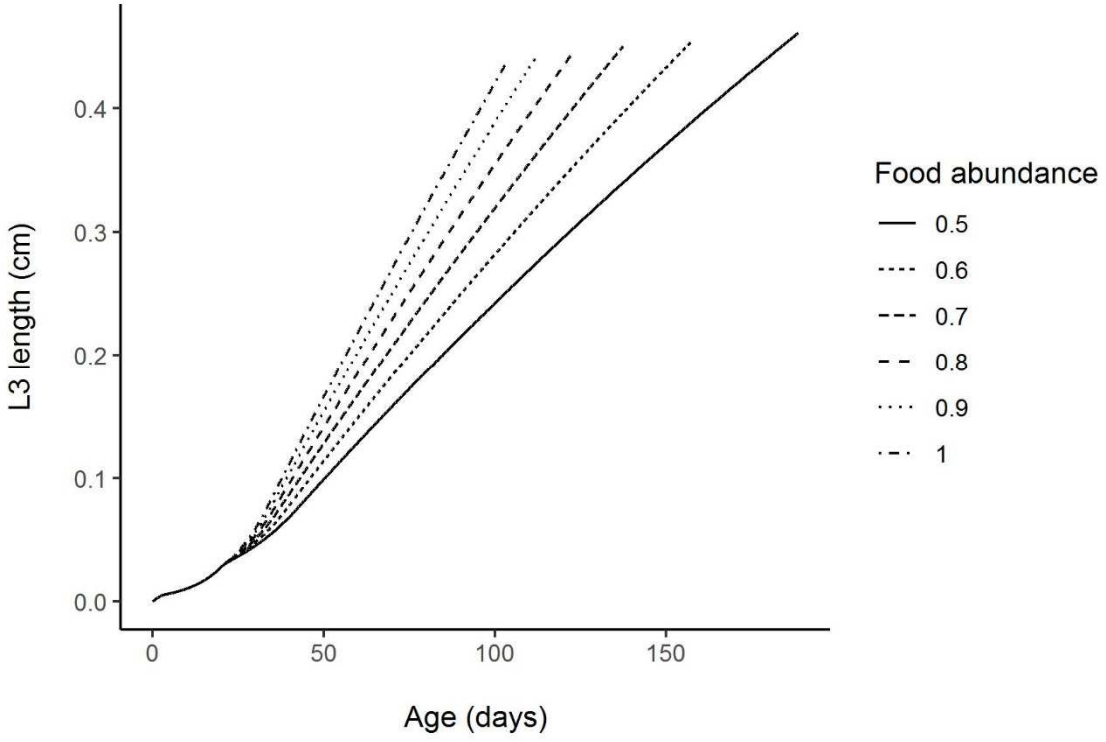

b)

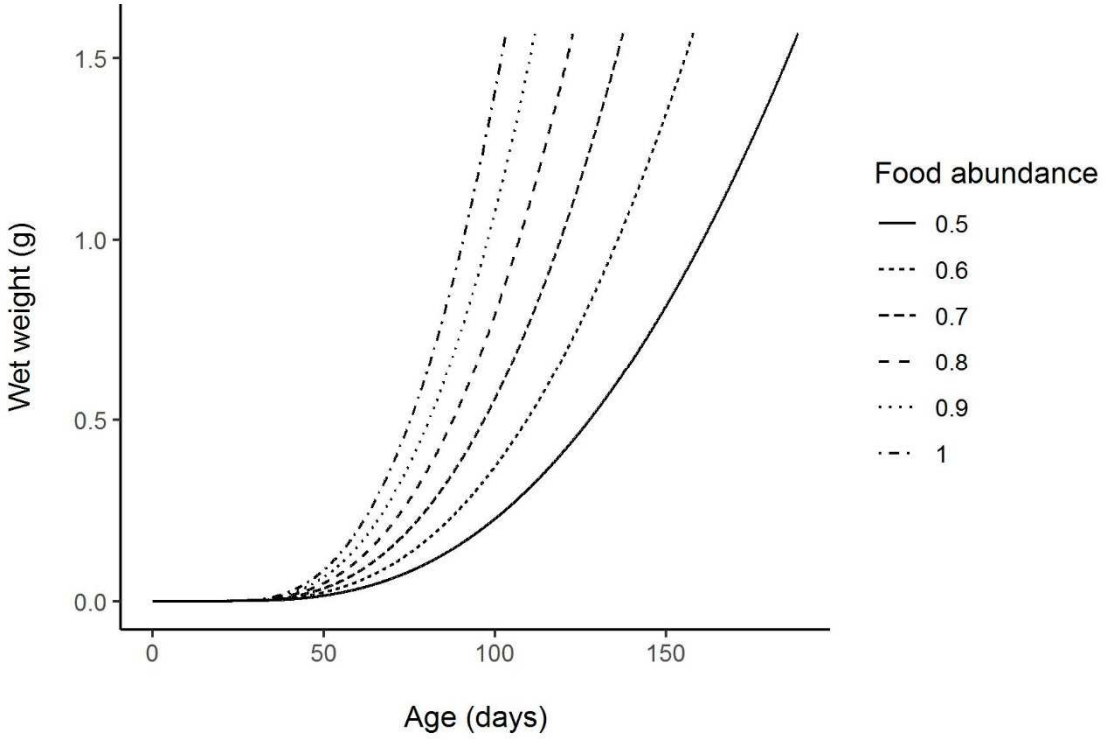

727 Table 1. DEB abj-model parameters estimated for the polychaete *Hediste diversicolor*
728 (Lefebvre, 2019, Add-my-Pet database).

729

Parameters	Value	Unit	Description
L_m	0.53073	Cm	Maximum volumetric length
$\{\dot{p}_{Am}\}$	14.3197	J cm^{-2} d^{-1}	Maximum surface-specific assimilation rate
$\dot{v}$	0.01123	cm d^{-1}	Energy conductance (velocity)
g	2.761754	-	Energy investment ratio
$\dot{k}_J$	0.002	d^{-1}	Maturity maintenance rate coefficient
$\dot{k}_M$	0.007663691	d^{-1}	Somatic maintenance rate
κ	0.96018	-	Allocation fraction to soma
κ_R	0.95	-	Reproduction efficiency
$[\dot{p}_M]$	25.91	J cm^{-3} d^{-1}	Volume specific somatic maintenance rate
$[E_G]$	3380.46	J cm^{-3}	Volume specific costs of structure
E_H^b	0.0003164	J	Energy maturity at birth
E_H^j	0.7665	J	Energy maturity at metamorphosis
E_H^p	7.883	J	Energy maturity at puberty
T_A	4877.15	K	Arrhenius temperature
T_{ref}	293.15	K	Reference temperature
ω	0.440695	-	Contribution of reserve to body weight or physical volume
δ_M	2.3579	-	Shape coefficient for L3 length
η_{OA}	0.329	µmol-O_2 J^{-1} d^{-1}	Energy-oxygen coupling coefficient for the assimilation flux
η_{OD}	1.977	µmol-O_2 J^{-1} d^{-1}	Energy-oxygen coupling coefficient for the dissipation flux
η_{OG}	0.285	µmol-O_2 J^{-1} d^{-1}	Energy-oxygen coupling coefficient for the growth flux
η_{NA}	0.045	µmol-NH_3 J^{-1} d^{-1}	Energy-ammonia coupling coefficient for the assimilation flux
η_{ND}	0.273	µmol-NH_3 J^{-1} d^{-1}	Energy-ammonia coupling coefficient for the dissipation flux
η_{NG}	0.039	µmol-NH_3 J^{-1} d^{-1}	Energy-ammonia coupling coefficient for the growth flux

730
731
732

733 Table 2. Growth performance of *Hediste diversicolor* fed with fish faeces and
734 commercial fish feed over time (age in days), and associated means of L3 length (cm),
735 wet weight (WW g) and survival: n = number of observations and SD = standard
736 deviation. Statistical analysis was performed with food type as fixed factor and tank as
737 random factor (* when $p < 0.05$).
738

Age (days)	Food type	n	L3 ± SD (cm)	WW ± SD (g)	Survival (%)
113	Fish faeces	54	0.11 ± 0.02		
	Fish feed	54	0.12 ± 0.02		
144	Fish faeces	50	0.21 ± 0.05		93
	Fish feed	52	0.18 ± 0.05		96
177	Fish faeces	45	0.30 ± 0.05*	0.35 ± 0.16	83
	Fish feed	42	0.27 ± 0.05*	0.30 ± 0.18	78
211	Fish faeces	31	0.30 ± 0.05	0.41 ± 0.17	57
	Fish feed	26	0.28 ± 0.06	0.36 ± 0.15	48

739
740
741

Table 3. Effects of temperature and scaled functional response (f=0.5, f=0.6 and f=1 at 20°C; 5°C and 25°C with f=1) on *H. diversicolor* L3 length (cm), wet weight (WW g) and total assimilated energy (Assim in J) and faeces assimilation (g DW). Total assimilated energy was estimated over ragworm production cycle (see Wang et al. 2020 for production cycle description). A production cycle was stopped when GSI reached 3%, or when WW reached 0.5 g WW (minimum polychaete market weight). The bioremediation capacity of one individual was estimated by transforming the assimilated energy in fish faeces by assuming (based on the literature) that 1 g of fish faeces represents 10.4 kJ. A population density of 3700 ind.m^{-2} (Scaps, 2002) was chosen to estimate the bioremediation capacity of a ragworm farm per m^2 and year.

T	**f**	**age**	**L3**	**WW**	**GSI**	**Surv**	**Assim (per ind.)**			**Bioremediation**	
(°C)		days	cm	g	%	%	J cycle^{-1}	J yr^{-1}	g (DW) yr^{-1}	g (DW) m^{-2} yr^{-1}	kg (DW) 100m^{-2} yr^{-1}
up to 3% GSI											
20	0.5	99	0.24	0.2	3.0	90	641	2370	0.23	755	75
20	1	79	0.31	0.6	3.0	90	1603	7443	0.72	2370	237
5	1	163	0.31	0.6	3.0	90	1596	3572	0.34	1137	114
25	1	64	0.31	0.6	3.0	90	1600	9067	0.87	2887	289
up to 0.5 g WW											
20	0.5	128	0.32	0.5	3.9	67	1536	4390	0.42	1039	104
20	1	75	0.30	0.5	2.9	90	1363	6598	0.63	2122	212
5	1	155	0.30	0.5	2.9	90	1355	3187	0.31	1025	103
25	1	62	0.30	0.5	2.9	90	1362	8020	0.77	2579	258